

Spatially limited antiferromagnetic order in a cluster glass compound $\text{Tb}_2\text{Ni}_{0.90}\text{Si}_{2.94}$

Santanu Pakhira^{a,b}, Chandan Mazumdar^{a,*}, Maxim Avdeev^{c,d}, R. N. Bhowmik^e, R. Ranganathan^a

^a*Condensed Matter Physics Division, Saha Institute of Nuclear Physics, 1/AF, Bidhannagar, Kolkata 700064, India*

^b*Ames Laboratory-USDOE and Department of Physics and Astronomy, Iowa State University, Ames, Iowa 50011, USA*

^c*Australian Nuclear Science and Technology Organisation, Locked Bag 2001, Kirrawee DC, New South Wales, 2232, Australia*

^d*School of Chemistry, The University of Sydney, Sydney, NSW, 2006, Australia*

^e*Department of Physics, Pondicherry University, R.V.Nagar, Kalapet, Pondicherry 605014, India*

Abstract

In the present study, the synthesis of a new ternary intermetallic compound $\text{Tb}_2\text{Ni}_{0.90}\text{Si}_{2.94}$ has been reported. The detailed studies on structure, static and dynamical magnetic properties of the compound have been investigated by means of powder x-ray diffraction, compositional analysis, dc & ac magnetization, non-equilibrium dynamics, heat capacity and neutron diffraction measurements. The dc & ac magnetic susceptibility reveal that the compound undergoes spin cluster-glass behaviour below 9.9 K. The frequency dependence of the freezing temperature have been analyzed on the basis of dynamic scaling laws such as power-law divergence and Vogel-Fulcher law, which further confirm the cluster-glass state formation for the compound. A detailed study on non-equilibrium dynamical behaviour associated with cluster-glass state has been carried out through magnetic relaxation behaviour along with magnetic memory effect in zero-field-cooled (ZFC) as well as field-cooled (FC) conditions and associated aging effect. The zero-field neutron diffraction study reveals the presence of a spatially limited antiferromagnetic phase in addition to the magnetically frustrated cluster-glass state. This result has also been supported through zero-field heat capacity studies. The variation in local electronic environment among the magnetic rare-earth ions caused by the structural disorder associated with Ni/Si ions have been argued to be responsible for the coexistence of different magnetic phases.

Keywords: Intermetallic, X-ray diffraction, Magnetization, Spin glass

*chandan.mazumdar@saha.ac.in

Email address: santanupakhira20006@gmail.com (Santanu Pakhira)

1. Introduction

In the last few decades, studies of magnetic ground state in different disordered systems have been regarded as an emerging research field involving several significant discoveries[1, 2, 3, 4]. The complex structure-property relationship in such systems have always stimulated condensed matter physicists and material scientists to develop a better understanding of experimentally observed many intriguing physical properties, which are radically different from that expected in conventional ordered systems. Spin-glass type systems are one such example where competition between disorder and magnetic frustration attributed to the competing interactions gives rise to exotic physical states which are of interest from fundamental physics point of view[1]. Additionally, observation of aging phenomena and magnetic memory effect in such systems, have found applications in more diverse fields, *e.g.*, in memory devices, applications to the artificial neural networks in computational science, *etc*[5, 6, 7]. Competition between disorder and magnetic interaction length scale in different magnetically frustrated glassy systems is always expected to reveal different new insights in this particular research area.

Ternary intermetallic $R_2\text{TSi}_3$ -type of systems, with R = rare-earth ions, T = transition metals, is one such prototype system that exhibits different complex low temperature magnetic phases including spin-glass phase[8, 9, 10, 11, 12, 13, 14, 15, 16, 17]. In these type of hexagonal systems (space group $P6/mmm$), competing exchange interaction arises due to the closeness of hexagonal lattice parameters. The random arrangement of T and Si atoms provide sufficient disorder to drive the ground state of many such systems into spin-freezing state in the presence of competing interaction. Recently, it is also reported that most of the isostructural $R_2\text{NiSi}_3$ -type of compounds could be synthesized in single phase by creating lattice vacancies in Ni and Si sites that is expected to introduce additional disorder in these systems[18, 19, 20, 21, 22, 23, 24]. It is known that depending on the disorder concentration in a magnetic system, long-range ordered magnetic ground state is tuned by the delicate balance of disorder content and percolation threshold for exchange pathways. As the amount of defects varies in different $R_2\text{NiSi}_3$ type compounds, magnetic interaction strength also varies abruptly in different rare-earth analogues of this series. For example, although both the full stoichiometric Gd_2NiSi_3 and Er_2NiSi_3 found to exhibit spin-glass state coupled with long range antiferromagnetic order, both the transition temperatures coincide in case of Gd-analogue but in the Er based compound spin freezing occurs below its Néel temperature[15]. Neutron diffraction further reveals that the antiferromagnetic coherence length in Er_2NiSi_3 is only $\sim 250\text{\AA}$ at 1.5 K, *i.e.*, ordering is confined up to about 60 crystal unit cells. The presence of disorder in $\text{Ho}_2\text{Ni}_{0.95}\text{Si}_{2.95}$ restricts the magnetic coherence length only up to 8 unit cells[18] and it is even much lower in case of Pr-based analogue. Thus, depending upon the disorder concentration and competing exchange interaction, the magnetic correlation length in these systems varies significantly, resulting the formation of coexisting multiple magnetic phases in these systems. In this work, we report the synthesis and physical properties of Tb-based analogue that also forms in single phase with defect crystal structure. We have shown that in the presence of strong disorder and competing exchange interaction, the compound exhibits spin freezing behavior coexisting with spatially

confined antiferromagnetic order at low temperatures.

2. Experimental details

Polycrystalline compounds were prepared by arc-melting technique using appropriate amount of Tb (metal ingot, phase purity 99.9%), Ni (metal slug, phase purity 99.98%) and Si (metal lump, phase purity 99.9999%). The mixture was remelted several times with intermediate flipping in order to achieve homogeneity. The phase nature of the resulting materials were determined by x-ray diffraction (XRD) experiments using Cu-K α radiation on a TTRAX-III diffractometer (M/s Rigaku, Japan). The structural characterization was done by Rietveld analysis of the powder XRD data using FULLPROF software package[25]. The chemical phase homogeneity was checked by scanning electron microscopy (SEM) measurements in the instrument EVO 18 (M/s Carl Zeiss, Germany) and the energy dispersive x-ray spectroscopy (EDX) measurements (M/s EDAX Inc., USA). Magnetization data were measured using SQUID magnetometer (M/s Quantum Design Inc., USA) and Ever Cool II VSM (M/s Quantum Design Inc., USA). Heat capacity data were collected with a Physical Properties Measurement System (PPMS) (M/s Quantum Design Inc., USA). Neutron diffraction measurements were carried out at ECHIDNA beamline in Australian Nuclear Science and Technology Organisation (ANSTO) for $\lambda = 2.4395\text{\AA}$.

3. Results and Discussions

3.1. Structural Characterization

The room temperature powder x-ray diffraction (XRD) data of as-cast full stoichiometric Tb₂NiSi₃ compound is presented in fig. 1(a). Most of the diffraction peaks in the experimentally observed XRD pattern can be indexed with AlB₂ type hexagonal crystal structure having space group *P6/mmm*. However, some additional peaks belonging to a secondary phase appear in the vicinity of most intense peak of Tb₂NiSi₃ phase (marked with '*'). The ICDD database coupled with PDXL software package reveals that the additional phase is of TbNiSi₂ type. However, we have earlier shown that by synthesizing different members of R₂NiSi₃ family of compounds with defect stoichiometry, single phase nature could be achieved. To achieve this, the fraction of TbNiSi₂ phase present in Tb₂NiSi₃ phase was determined first. In the next step, the amount of Tb, Ni, Si responsible for such 1:1:2 phase formation was removed from the 2:1:3 phase, that essentially results in a defect stoichiometry. In this way, the single phase nature is achieved for this compound with nominal stoichiometry Tb₂Ni_{0.90}Si_{2.94}. The Rietveld refinement using FullProf software package confirms the single phase nature of the compound with calculated stoichiometry Tb₂Ni_{0.91(1)}Si_{2.95(1)} and lattice parameter values $a = 3.968(1)\text{\AA}$ and $c = 4.054(1)\text{\AA}$ (Table 1). Similar to isostructural compounds, the ratio, c/a ($= 1.021$), is close to unity for this compound. Chemical phase homogeneity of the prepared as-cast sample was further investigated through scanning electron microscopy (SEM) measurements both in back-scattered electron detector (BSE) mode and secondary electrons (SE) mode. The SE image and elemental mapping through EDX measurements reveal single phase nature of the material with average stoichiometry

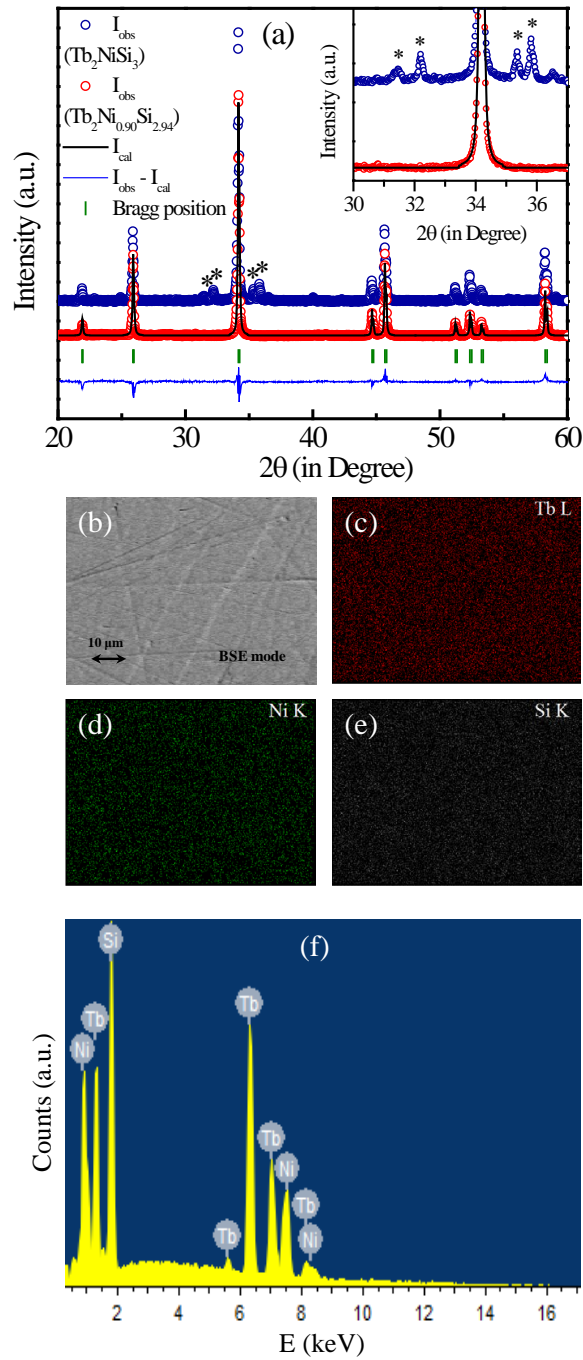


Figure 1: (a) Powder XRD pattern of Tb_2NiSi_3 taken at room temperature is shown by blue symbol. The prominent secondary peaks are marked with '*'. Rietveld fit of the powder XRD pattern of $\text{Tb}_2\text{Ni}_{0.90}\text{Si}_{2.94}$ taken at room temperature is shown in black line. The blue difference curve corresponds for $\text{Tb}_2\text{Ni}_{0.90}\text{Si}_{2.94}$ compound. Inset shows zoomed-in 2θ region around the most intense peak. SEM picture taken in BSE mode from the polished surface of $\text{Tb}_2\text{Ni}_{0.90}\text{Si}_{2.94}$ is shown in (b). Fig.(c)-(e) shows elemental mapping obtained from SEM image. (f) Elemental analysis of the EDX spectrum.

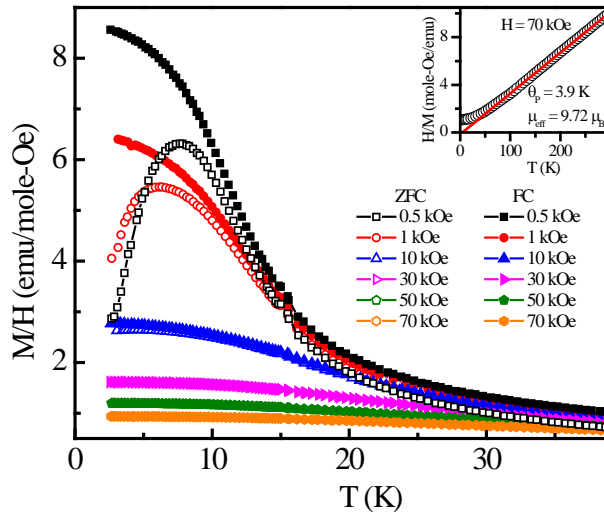


Figure 2: $M(T)$ behaviour at different applied magnetic fields under ZFC and FC conditions. Temperature variation of Inverse susceptibility (H/M) behaviour along with linear Curie-Weiss fit is shown in inset.

$Tb_2Ni_{0.89(3)}Si_{2.96(2)}$, which is quite close to that obtained from Rietveld refinement. The uniform contrast of the SEM image taken in BSE mode conforms the phase homogeneity of the synthesized material.

Table 1: Crystallographic and refinement parameters obtained from the structural analysis of room temperature powder x-ray diffraction data of $Tb_2Ni_{0.90}Si_{2.94}$.

Lattice parameters					
	$a(\text{\AA})$				3.968(1)
	$c(\text{\AA})$				4.054(2)
	$c(\text{\AA})/a(\text{\AA})$				1.021(1)
	$V_{\text{cell}} (\text{\AA}^3)$				55.291(2)
Refinement quality					
	χ^2				4.1
	R_f (%)				7.9
	R_{Bragg} (%)				10.3
Atomic coordinates					
Atom	Wyckoff Symbol	x	y	z	occupancy (%)
Tb	$1a$	0	0	0	100
Ni	$2d$	1/3	2/3	1/2	22.75(20)
Si	$2d$	1/3	2/3	1/2	73.75(30)

3.2. Static magnetization

Fig. 2 displays temperature dependence of zero-field-cooled (ZFC) and field-cooled (FC) dc magnetization for different applied magnetic fields. As can be seen from the figure, for low applied magnetic field, ZFC magnetization exhibits an extended cusp below 9 K that shifts to lower temperature with increasing magnetic field strength. In those applied field

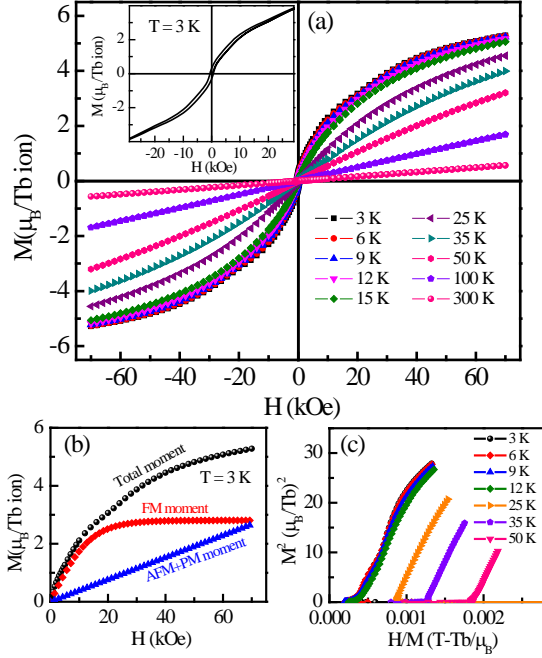


Figure 3: Magnetic field dependence of isothermal magnetization at different temperatures. Inset shows $M(H)$ at $T = 3$ K. (b) $M(H)$ behaviour for magnetic field change $0 \rightarrow 70$ kOe along with decoupled moment contribution according to Eq. 1. (c) Arrott plots (H/M vs M^2) using $M(H)$ data at different temperatures.

region, the magnetization behaviour remarkably varies depending on the ZFC and FC protocols. The FC magnetization curve for 0.5 kOe applied magnetic field strength deviates considerably from the ZFC behaviour below 12 K. The ZFC cusp broadens further with increase in magnetic field strength and merges with FC magnetization for magnetic field strength beyond 10 kOe. Such type of smeared peaks in ZFC magnetization and bifurcation between ZFC and FC magnetization from well above the peak temperature is typically observed in many glassy and superparamagnetic systems due to the presence of large distribution of cluster sizes[26, 27]. The effective magnetic moment and the paramagnetic Curie temperature were estimated by fitting the temperature dependence of inverse susceptibility behaviour with linear Curie-Weiss behaviour in the temperature range 120 K - 300 K, and founds to be $\mu_{\text{eff}} = 9.72 \mu_B/\text{Tb-ion}$ and $\theta_p = 3.9$ K [Inset (II): Fig. 2]. The obtained effective moment value signifies that, it is primarily the localized rare-earth ion moment, that is responsible for magnetic contribution in the system. The positive value of θ_p further yields the presence of considerable ferromagnetic interaction in the system, although the magnetic susceptibility does not indicate the presence of any long-range ferromagnetic or even anti-ferromagnetic ordering. However, the estimation of small value of θ_p in comparison to any possible phase transition points towards the presence of competing magnetic interaction in the compound[18].

The magnetic hysteresis loops measured at different temperatures for $\text{Tb}_2\text{Ni}_{0.90}\text{Si}_{2.94}$ is depicted in Fig. 3(a). The magnetic isotherms exhibit weak hysteresis behaviour for $T = 3$ K and 6 K. However, in all other measured temperatures, no sign of magnetic hysteresis

is observed. The value of coercivity (~ 590 Oe) and remanence ($0.3 \mu_B/\text{Tb ion}$) founds to be quite small even at the lowest measured temperature, 3 K. Though magnetic isotherms at lower temperatures tend to saturate at higher applied magnetic fields, the magnetization value at 2 K for 70 kOe magnetic field is $5.3 \mu_B$, which is much below the calculated value of $gJ = 9\mu_B$. The absence of magnetic saturation and weak hysteresis behaviour signifies the presence of glassy phase in the system due to competing ferromagnetic and antiferromagnetic exchange interaction[28]. The field dependence of low temperature magnetic isotherms also can not be solely described by the tangent-hyperbolic of Brillouin function, that is commonly used to describe the ferromagnetic behaviour in a system. Rather, as seen from the Fig. 3(b), it can be best described by the following equation[18, 29],

$$M(H) = A[\tanh(BH)] + CH \quad (1)$$

where the linear term arises due to the presence of antiferromagnetic and (or) paramagnetic interaction in the system. This type of analysis further reveal the presence of competing exchange interaction in the system. Fig. 3(c) depicts the Arrott plot[30], where M^2 is plotted as a function of H/M for the same set of isothermal magnetization curves. No signature of spontaneous magnetization could be observed, further confirming the presence of short range magnetic ordering in the system and also indicate towards glassy magnetic transitions[31, 32]. It may be noted that the $M(H)$ isotherms for the temperatures 9 K-50 K showed non-linear behaviour, which is typical characteristics of short-ranged magnetic spin order/clustering in the paramagnetic state.

3.3. Dynamical susceptibility and scaling

To obtain further information about the low temperature magnetic ground state of $\text{Tb}_2\text{Ni}_{0.90}\text{Si}_{2.94}$, ac susceptibility measurements have been carried out at different frequencies. Fig.4(a) and (b) shows the temperature dependence of real (χ') and imaginary (χ'') part of ac susceptibility, respectively. The $\chi'(T)$ exhibits a pronounced peak around 9.9 K for 37.7 Hz which is often used to define the spin freezing temperature (T_f) and shifts to higher temperature with the increase in ac frequency. $\chi''(T)$ also exhibits well defined peak at slightly lower temperature, that also exhibit frequency dependence. The magnitude of $\chi''(T)$ that is related to dissipation process in a system increases with increase in frequency. It may be mentioned here that, for an ideal ferromagnetic system the magnitude of $\chi''(T)$ sharply decreases for temperatures below and above the temperature which also happen to be frequency independent[2, 33]. The non-zero value of $\chi''(T)$ around T_f in $\text{Tb}_2\text{Ni}_{0.90}\text{Si}_{2.94}$ may be either due to spin freezing behaviour or superparamagnetic blocking[1, 34]. To remove the ambiguity, the frequency dependence of shift of $\chi'(T)$ has been determined by employing the quantity[1],

$$\delta T_f = \frac{\Delta T_f}{T_f \Delta(\log_{10} \nu)} \quad (2)$$

and estimated to be 0.09. The value is an order of magnitude larger than those reported for different canonical SG systems e.g. CuMn ($\delta T_f = 0.0045$)[1], AuMn ($\delta T_f = 0.0045$)[35] and also one order of magnitude smaller than that generally observed in various superparamagnets e.g. Mn/CdSe Quantum Dots ($\delta T_f = 0.16$)[36], $\alpha\text{-[Ho}_2\text{O}_3(\text{B}_2\text{O}_3)]$ ($\delta T_f = 0.28$)[1], etc.

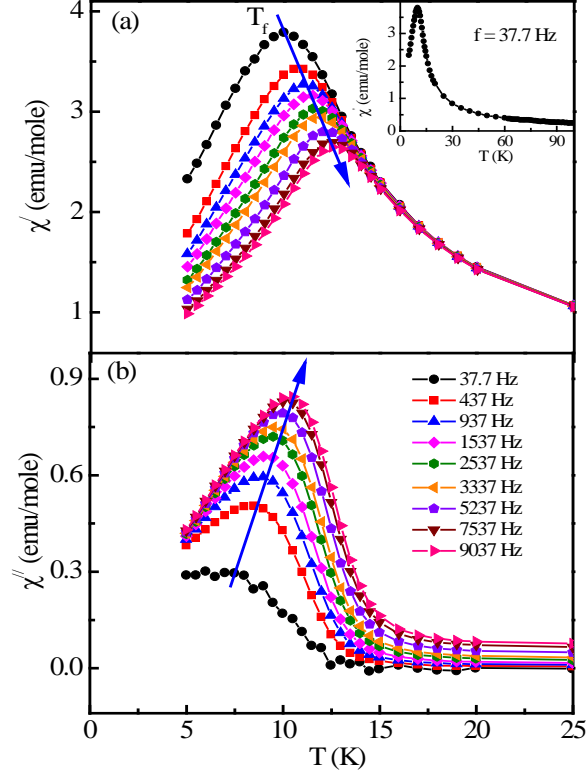


Figure 4: Temperature dependence of (a) in-phase component (χ') and (b) out-of-phase component (χ'') of ac susceptibility at different frequencies. Inset of (a) shows in-phase component for 37.7 Hz in a wider temperature scale.

The value of δT_f in $\text{Tb}_2\text{Ni}_{0.90}\text{Si}_{2.94}$ is comparable to those reported for different cluster-glass systems reported earlier[1, 38, 39]. It may however be noted that, it may not be wise to conclude whether a system is glassy system or a superparamagnetic one, solely from the value of δT_f (sometimes called Mydosh parameter).

Therefore, to understand further the nature of glassy phase, we have attempted to analyse the relaxation time behaviour of the system using the Arrhenius relation[34],

$$\tau = \tau_0 \exp\left(-\frac{E_a}{k_B T}\right) \quad (3)$$

where, τ_0 is inverse of characteristic attempt frequency, E_a is activation energy and k_B is the Boltzman constant. In general, the relaxation time in different superparamagnetic systems are known to follow the above mentioned Arrhenius relation[34]. However, as seen from Fig. 5(a) the $\log \tau$ vs $1/T$ behaviour deviates significantly from the linear behaviour which further rules out the possibility of superparamagnetic blocking in $\text{Tb}_2\text{Ni}_{0.90}\text{Si}_{2.94}$. Furthermore, the relaxation behaviour in $\text{Tb}_2\text{Ni}_{0.90}\text{Si}_{2.94}$ can be well described by empirical Vogel-Fulcher relation, proposed for magnetically interacting clusters, of the form[1, 40],

$$\tau = \tau_0 \exp\left(\frac{E_a}{K_B(T_f - T_0)}\right) \quad (4)$$

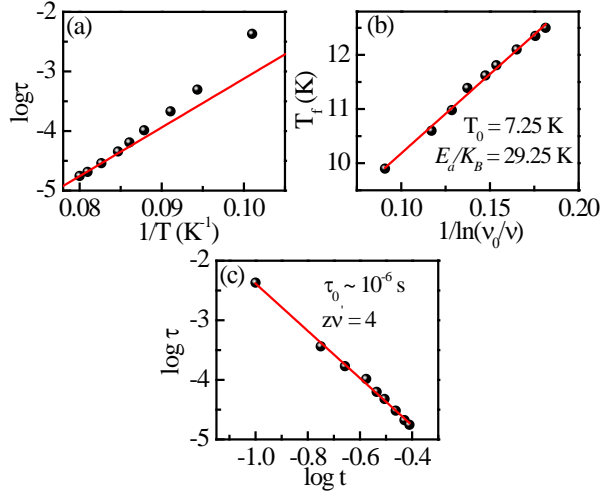


Figure 5: (a) Logarithm (base-10) of the time scale associated with measured frequency ($\tau = 1/f$) as a function of the inverse of the peak temperature in $\chi'(T)$. The solid line is fit to Eq. 3. (b) T_f as a function of $1/\ln(\nu_0/\nu)$ and fit to Eq. 5 is shown by solid line. (c) The variation of $\log \tau$ as a function of logarithmic of reduced temperature t (discussed in text). The solid line represents fit according to Eq. 6.

In terms of frequency, Eq. 4 can be written as,

$$\nu = \nu_0 \exp\left(-\frac{E_a}{K_B(T_f - T_0)}\right) \quad (5)$$

where T_0 is the Vogel-Fulcher temperature. The value of the ratio $\frac{E_a}{K_B}$ and T_0 have been determined from the linear fit of T_f vs $1/\ln(\nu_0/\nu)$ (Fig. 5(b)) and found to be 29.25 K and 7.25 K, respectively. Thus our analysis rather favours the development of cluster-glass state in this system[20, 21, 41].

In different spin-glass systems, temperature dependence of relaxation time exhibits critical slowing down behaviour and can be expressed by the power law[42],

$$\tau = \tau_0 \left(\frac{T_f - T_{SG}}{T_{SG}}\right)^{-z\nu'} \quad (6)$$

where τ_0 is microscopic single spin flipping time, $z\nu'$ is critical exponent, and T_{SG} is the spin freezing temperature in static limit ($f \rightarrow 0$). Though few earlier studies have chosen T_{SG} to be temperature at which the ZFC dc magnetization curve has its maximum for the sake of simplicity[43], we have estimated the value of T_{SG} by extrapolating the $T_f(\nu)$ data in the $\nu \rightarrow 0$ limit[38] and found to be 9.0(1) K. We have also determine the value of T_{SG} by choosing the temperature required for the best fit to Eq. 6 that minimized the least square deviation from a straight line fit and estimated to be 9.1(1) K, which is almost same to 9.0(1) mentioned above. The linear fit of $\log(\tau) - \log(t)$ dependence, with $t = \frac{T_f - T_{SG}}{T_{SG}}$ yields, τ_0 of the order of 10^{-6} s and $z\nu' = 4.0(2)$. The intrinsic relaxation time τ_0 is found to be similar to those observed in different cluster-glass systems[1]. All these dynamical scaling parameter values confirms the cluster-glass behaviour in $\text{Tb}_2\text{Ni}_{0.90}\text{Si}_{2.94}$ where interacting magnetic clusters freeze below T_f .

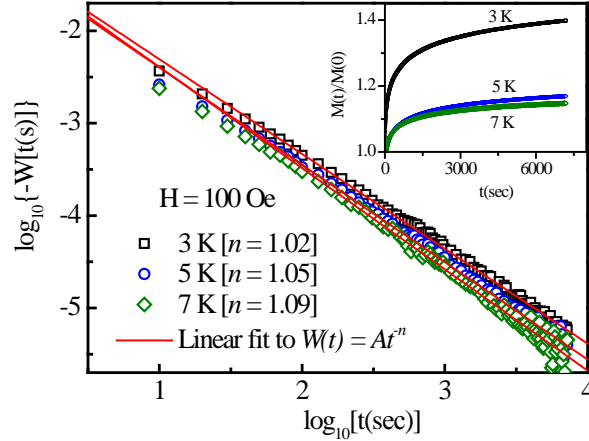


Figure 6: Relaxation rate at different temperatures below T_f for a constant magnetic field exposure of 100 Oe. Inset shows the corresponding relaxation behaviour in ZFC mode.

3.4. Non-equilibrium dynamics

Evidence for cluster-glass state formation has also been provided on the basis of temperature dependent magnetic relaxation behaviour in the studied $Tb_2Ni_{0.90}Si_{2.94}$ system. Inset of Fig. 6 shows the magnetic relaxation behaviour in ZFC mode at three temperatures viz., 3 K, 5 K, and 7 K, below T_f for 100 Oe applied magnetic field strength. In ZFC procedure, the sample was initially cooled down the measured temperature in the absence of any magnetic field. After time lapse for 60 sec, needed for temperature stabilization, 100 Oe magnetic field was applied (at a sweep rate of 50 Oe/sec) and $M(t)$ behaviour was recorded. The observation time count starts ($t = 0$) as soon as the recording of $M(t)$ data was started after the magnetic field reach 100 Oe. The relaxation rate depends on the interaction strength of the magnetic clusters take part in the relaxation process and Ulrich *et al.*[44] have shown that it decays following the power law,

$$W(t) = At^{-n}, t \geq t_0 \quad (7)$$

where, $W(t) = -(d/dt)[\ln m(t)]$ ($m(t) = M(t)/M(t = 0)$), and A is fitting parameter. As seen from Fig. 6, the value of n , which depends on the inter-cluster strength is not constant but varies over different temperatures below T_f . Furthermore, the values are very close to 1 signifying a strong interaction among the magnetic clusters in the system. Thus, temperature dependent magnetic relaxation behaviour in $Tb_2Ni_{0.90}Si_{2.94}$ further confirms spin cluster-glass state formation.

Since the spin-glass or cluster-glass state is a non-equilibrium state, the aging phenomena generally considered to be a key signature of non-equilibrium dynamical behaviour in different glassy systems[45, 46, 47]. Different spin-glass type of systems are known to keep memory of their previous state history due to non-ergodicity in the system. To examine the aging behaviour in $Tb_2Ni_{0.90}Si_{2.94}$, magnetic memory effect has been studied under both FC and ZFC configurations following the protocol suggested earlier by Sun *et al.*[48]. In FC method, the sample was cooled down to the lowest temperature, 2 K, from the paramagnetic

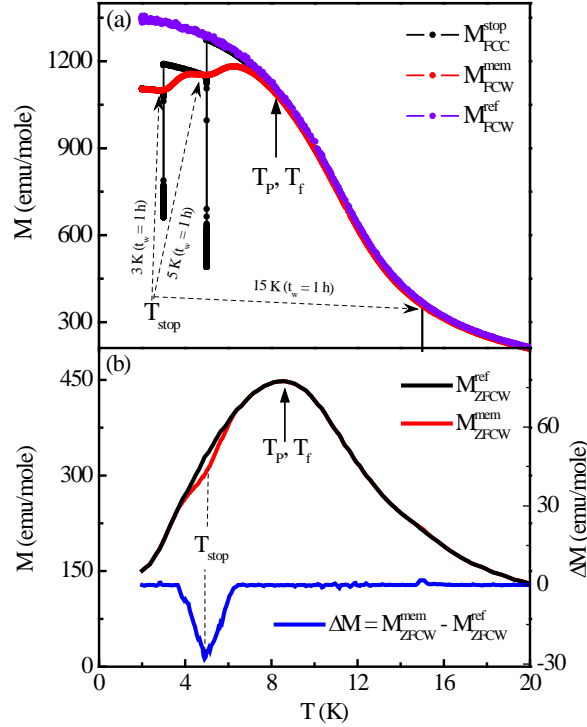


Figure 7: Magnetic memory effect in (a) FC and (b) ZFC protocol.

region under 100 Oe applied magnetic field at a constant temperature sweep rate (1 K/min) with some intermediate stops at T_{stop} of duration 1 h (t_w) (Fig. 7(a)). The magnetic field was switched off during the time duration t_w , allowing the system to relax and was switched on again after the wait time, followed by cooling process. The $M(T)$ behaviour obtained in this process is referred as $M_{\text{FCC}}^{\text{stop}}$ that shows a step-like behaviour. The magnetization measured during the heating process, $M_{\text{FCW}}^{\text{mem}}$ attempt to follow the past history of $M_{\text{FCC}}^{\text{stop}}$ exhibiting the memory effect. $M_{\text{FCW}}^{\text{ref}}$ is the conventional FC magnetization curve that does not involve such intermediate stops in measurements. In ZFC method, the sample was cooled to 2 K from the paramagnetic region in the absence of any magnetic field with a intermediate stop at 5 K (T_{stop}) of time period 1 h (t_w). $M(T)$ behaviour was measured during the heating cycle under the exposure of 100 Oe magnetic field and the data obtained is labeled as $M_{\text{ZFCW}}^{\text{mem}}$ which significantly deviate from conventional ZFC magnetization behaviour ($M_{\text{ZFCW}}^{\text{ref}}$) close to T_{stop} , as can be clearly visualized from the difference in magnetization curve (Fig. 7(b)). The presence of ZFC memory effect establishes the cluster-glass behaviour in $\text{Tb}_2\text{Ni}_{0.90}\text{Si}_{2.94}$ instead of the non-interacting blocking behaviour generally observed in superparamagnetic materials[48, 49, 50, 51]. This type of observed magnetic memory effect supports the aging behaviour of the system associated with cluster glass state formation.

3.5. Heat capacity

In order to get further insight into the low temperature magnetic state formation, zero-field heat capacity data measurements were carried out for $\text{Tb}_2\text{Ni}_{0.90}\text{Si}_{2.94}$ and isostructural

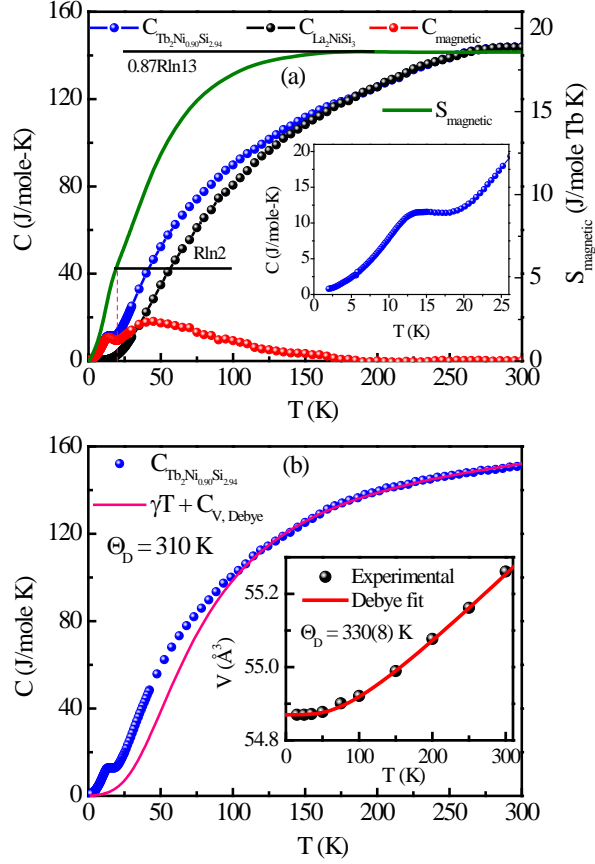


Figure 8: (a) (Left panel) Zero field heat capacity, $C(T)$ of $\text{Tb}_2\text{Ni}_{0.90}\text{Si}_{2.94}$ and nonmagnetic analog La_2NiSi_3 in the temperature range 2-300 K. The estimated magnetic contribution of heat capacity (C_{magnetic}) is also shown. (Right panel) Calculated magnetic entropy (S_{magnetic}) from C_{magnetic} behaviour is presented as a function of temperature. (b) $C(T)$ along with fit to Debye model of specific heat (Eq. 9). Inset shows temperature dependence of lattice unit cell volume with fit to corresponding Debye model.

non-magnetic analogue La_2NiSi_3 (Fig. 8(a)). No sharp peak (λ or Δ -like) due to a typical long-range magnetic transition is observed down to 2 K. Rather, a broad peak appears shouldered around 10 K (Inset: Fig. 8(a)). Estimation of the magnetic specific heat (C_{magnetic}) was done by subtracting the $C(T)$ data of La_2NiSi_3 from that of the $\text{Tb}_2\text{Ni}_{0.90}\text{Si}_{2.94}$ after normalization with lattice volume correction by scaling the T -axis of La -analogue using the relation[52],

$$T' = \frac{T}{\sqrt{FW_{\text{Tb}_2\text{Ni}_{0.90}\text{Si}_{2.94}}/FW_{\text{La}_2\text{NiSi}_3}}} \quad (8)$$

Upon subtraction of this estimated lattice contribution, a broad hump centered around 10 K is observed in the temperature dependence of C_{magnetic} data, which is characteristically similar to that generally observed around T_f for different spin-glass type of systems coupled

with magnetic ordering having very limited coherence length. The additional broader hump in the high temperature region of C_{magnetic} might be due to the Schottky anomaly associated with the crystalline electric field (CEF) level splitting in the compound. The high temperature heat capacity data of $\text{Tb}_2\text{Ni}_{0.90}\text{Si}_{2.94}$ was modeled by empirical Debye equation of the form,

$$C_P(T) = \gamma_T + 9nR \left(\frac{T}{\Theta_D} \right)^3 \int_0^{\Theta_D/T} \frac{x^4 e^x}{(e^x - 1)^2} dx \quad (9)$$

with Debye temperature, $\Theta_D = 310$ K (Fig. 8(b)). This value is in the same range to the Debye temperature estimated from the temperature dependence of unit cell volume[15, 53] of $\text{Tb}_2\text{Ni}_{0.90}\text{Si}_{2.94}$, where Θ_D founds to be 330(8) K (Inset: Fig. 8(b)). The estimated magnetic entropy (S_{magnetic}) founds to saturate above 150 K to a value 18.6 J/mole-Tb-K which is about 90% of $R \ln(2J+1)$, with $J = 6$ for Tb^{3+} ion. Thus, a considerable amount of magnetic entropy is frozen out at low temperatures that may be attributed to the presence of short-range magnetic correlation and (or) due to CEF level splitting. However, the value of S_{magnetic} around T_f found to be only 2.4 J/mole-Tb-K which is smaller than $R \ln 2$, for this non-Kramer ion (Tb: even J value) system. The broad peak in heat capacity data of $\text{Tb}_2\text{Ni}_{0.90}\text{Si}_{2.94}$ around T_f and low value of magnetic entropy further suggest that besides the spin freezing process if there is any additional magnetic order present in the system, that must be of finite correlation length.

3.6. Neutron diffraction studies

The zero field neutron diffraction measurements have been carried out to understand the nature of magnetic interactions in $\text{Tb}_2\text{Ni}_{0.90}\text{Si}_{2.94}$. Fig. 9(a)-(b) show the neutron diffraction pattern taken at 50 K and 1.7 K, respectively. The diffraction pattern for 50 K reveals that all the Bragg peaks can be indexed with nuclear structure. On the other hand, in case of 1.7 K pattern, the observation of a few additional peaks having substantially weak intensity indicates the presence of antiferromagnetic type interaction in the system at lower temperature (below 10 K). However, our attempt to determine the magnetic structure from the neutron diffraction patterns did not yield satisfactory results, due to the presence of preferred crystalline orientations (particularly in case of (1 1 2) plane) present in the as-cast lump shaped samples used in our measurements. Although the nuclear structure can be analysed by considering the preferred orientation effects, the presence of it however restricts the determination of magnetic structure as the magnetic domains may not be necessarily textured in the same way. Nonetheless, the magnetic correlation length have been estimated for the system from the full width at half maxima (FWHM) of the weak intensity magnetic peaks after considering the instrument resolution function and it appears to be only 40 Å at $T = 1.7$ K. The very short magnetic correlation length signifies a highly restricted spatial nature of antiferromagnetic interaction present in the system.

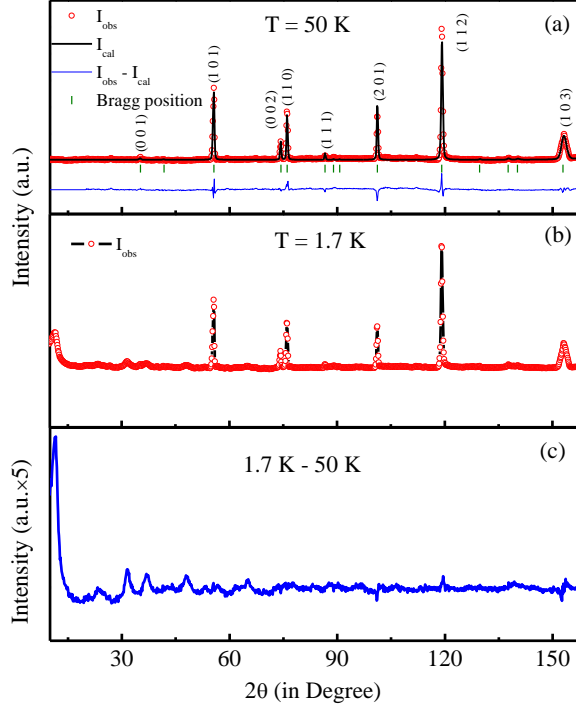


Figure 9: Zero field neutron diffraction pattern of $\text{Tb}_2\text{Ni}_{0.90}\text{Si}_{2.94}$ at (a) $T = 50$ K and (b) $T = 1.7$ K. (c) The magnetic part of the diffraction pattern for $T = 1.7$ K.

4. Summary

In summary, we report the successful synthesis of a new intermetallic compound $\text{Tb}_2\text{Ni}_{0.90}\text{Si}_{2.94}$ that forms in single phase only in defect structure, very similar to that earlier observed in many members of $R_2\text{Ni}_{1-\delta_1}\text{Si}_{3-\delta_2}$ (δ 's are very small positive fractional numbers) series of compounds. A bifurcating nature of dc magnetic susceptibility at low temperatures and in low field in ZFC and FC protocols suggest the presence of magnetic irreversibility in this system. AC magnetic susceptibility measurements suggests that the magnetic irreversibility likely to have originated from a cluster-glass state formation below 9.9 K in this compound. The presence of cluster-glass like phase has also been established through the detailed non-equilibrium dynamical studies. Neutron diffraction measurements indicate the presence of an additional antiferromagnetic type interactions of very short coherence length, ~ 40 Å at $T = 1.7$ K. The heat capacity measurement is also in agreement with the neutron diffraction result. The magnetic ground state of $\text{Tb}_2\text{Ni}_{0.90}\text{Si}_{2.94}$ thus appears to consist of at least two different magnetic phases: one glassy magnetic phase and another short-range ordered antiferromagnetic phase.

Acknowledgement

This work has been carried out and supported through CMPID-DAE project at SINP. The authors are thankful to Neetika Sharma for useful discussions during data analysis. The

authors are grateful to Tridib Das and Shibasis Chatterjee for SEM and EDX measurements. We also acknowledge the support and encouragement by Robert Robinson during the neutron diffraction experiments at ECHIDNA beamline at ANSTO in Australia. SP acknowledges the receipt of fellowship from Ames Laboratory-USDOE and Department of Physics and Astronomy, Iowa State University, USA.

References

- [1] J. A. Mydosh, *Spin glasses: An experimental introduction* (eds Taylor & Francis) (London, Washington, 1993).
- [2] K. Binder and A. P. Young, *Rev. Mod. Phys.* 58 (1986) 801.
- [3] K. Binder and W. Kob, *Galssy Materials and Disordered Solids* (eds World Scientific) (Singapore, 2005).
- [4] A. P. Ramirez, *Handbook of magnetic materials*, edited by K. H. J. Buschow, Vol. 13, ch. 4, (Elsevier, Amsterdam, 2001).
- [5] D. J. Amit, H. Gutfreund, and H. Sompolinsky, *Phys. Rev. A* 32 (1985) 1007.
- [6] S. Kirkpatrick, C. D. Gelatt and M. P. Vecchi, *Science* 220 (1983) 671.
- [7] D. L. Stein, *Proc. Natl. Acad. Sci. U. S. A* 82 (1985) 3670.
- [8] R. A. Gordon, C. J. Warren, M. G. Alexander, F. J. DiSalvo, and R. Pöttgen, *J. Alloys Comp.* 248 (1997) 24.
- [9] C. Tien, C. H. Feng, C. S. Wur, and J. J. Lu, *Phys. Rev. B* 61 (2000) 12151.
- [10] E. V. Sampathkumaran, H. Bitterlich, K. K. Iyer, W. Löser, and G. Behr, *Phys. Rev. B* 66 (2002) 052409.
- [11] D. X. Li, S. Nimori, Y. Shiokawa, Y. Haga, E. Yamamoto, and Y. Onuki, *Phys. Rev. B* 68 (2003) 012413.
- [12] M Frontzek, A Kreyssig, M Doerr, A Schneidewind, J-U Hoffmann, and M Loewenhaupt, *J. Phys: Cond. Mat* 19 (2007) 145276.
- [13] M. Szlawska, D. Kaczorowski, and M. Reehuis, *Phys. Rev. B* 81 (2010) 094423.
- [14] D. Gnida, M. Szlawska, P. Swatek and D. Kaczorowski, *J. Phys.: Condens. Matter* 28 (2016) 435602.
- [15] S. Pakhira, C. Mazumdar, R. Ranganathan, S. Giri, and M. Avdeev, *Phys. Rev. B* 94 (2016) 104414.
- [16] Z. J. Mo, J. Shen, X. Q. Gao, Y. Liu, C. C. Tang, J. F. Wu, F. X. Hu, J. R. Sun, B. G. Shen, *J. Alloys Comp.* 626 (2015) 145.
- [17] M. Szlawska, and D. Kaczorowski, *Phys. Rev. B* 84 (2011) 094430.
- [18] S. Pakhira, C. Mazumdar, R. Ranganathan, and M. Avdeev, *Sci. Rep.* 7 (2017) 7367.
- [19] S. Pakhira, C. Mazumdar, and R. Ranganathan, *J. Phys.: Condens. Matter* 29 (2017) 505801.
- [20] S. Pakhira, C. Mazumdar, R. Ranganathan, S. Giri, *J. Alloys Comp.* 742 (2018) 391.
- [21] S. Pakhira, C. Mazumdar, R. Ranganathan, S. Giri, *Phys. Chem. Chem. Phys.* 20 (2018) 7082.
- [22] S. Pakhira, C. Mazumdar, D. Choudhury, R. Ranganathan, S. Giri, *Phys. Chem. Chem. Phys.* 20 (2018) 13580.
- [23] S. Pakhira, C. Mazumdar, and R. Ranganathan, *J. Phys.: Condens. Matter* 30 (2018) 215601.
- [24] S. Pakhira, C. Mazumdar, A. Basu, R. Ranganathan, R.N. Bhowmik, and B. Satpati, *Sci. Rep.* 8 (2018) 14870.
- [25] Rodríguez-Carvajal, *J. Physica B* 192 (1993) 55.
- [26] A. K. Pramanik, and A. Banerjee, *Phys. Rev. B* 82 (2010) 094402.
- [27] A. Kumar, S. D. Kaushik, V. Siruguri, and D. Pandey, *Phys. Rev. B* 97 (2018) 104402.
- [28] X. Bie, Y. Wei, L. Liu, K. Nikolowski, H. Ehrenberg, H. Chen, C. Wang, G. Chen, F. Du, *J. Alloys Comp.* 551 (2013) 37.
- [29] K. Das, P. Dasgupta, A. Poddar & I. Das, *Sci. Rep.* 6 (2016) 20351.
- [30] A. Arrott, *Phys. Rev.* 108 (1957) 1394.
- [31] R. Mathieu, P. Nordblad, D.N.H. Nam, N.X. Puc, N.C. Khiem, *Phys. Rev. B* 63 (2001) 174405.

- [32] A. Kumar, R.P. Tandon, and V.P.S. Awana, *Eur. Phys. J. B* 85 (2012) 238.
- [33] A. A. Belik and E. Takayama-Muromachi, *Inorg. Chem.* 45 (2006) 10224.
- [34] S. Bedanta and W. Kleemann, *J. Phys. D: Appl. Phys.* 42 (2009) 013001.
- [35] C. A. M. Mulder, A. J. van Duynveldt, and J. A. Mydosh, *Phys. Rev. B* 25 (1982) 515.
- [36] D. Magana, S. C. Perera, A. G. Harter, N. S. Dalal, and G. F. Strouse, *J. Am. Chem. Soc.* 128 (2006) 2931.
- [37] J. Liu, Y. Mudryk, J.D. Zou, V.K. Pecharsky, K.A. Gschneidner Jr., *J. Alloys Comp.* 600 (2014) 101.
- [38] V. K. Anand, D. T. Adroja, and A. D. Hillier, *Phys. Rev. B.* 85 (2012) 014418.
- [39] P. Bag, P. R. Baral, and R. Nath, *Phys. Rev. B.* 98 (2018) 144436.
- [40] J. L. Tholence, *Solid State Commun.* 35 (1980) 113.
- [41] Y.J. Zhang, Q.Q. Zeng, Z.Y. Wei, Z.P. Hou, Z.H. Liu, E.K. Liu, X.K. Xi, W.H. Wang, X.Q. Ma, and G.H. Wu, *J. Alloys Comp.* 749 (2018) 134.
- [42] P. C. Hohenberg and B. I. Halperin, *Rev. Mod. Phys.* 49 (1977) 435.
- [43] A. Malinowski, V. L. Bezusyy, R. Minikayev, P. Dziawa, Y. Syryanyy, and M. Sawicki, *Phys. Rev. B.* 84 (2011) 024409.
- [44] M. Ulrich, J. García-Otero, J. Rivas, and A. Bunde, *Phys. Rev. B.* 67 (2003) 024416.
- [45] P. Granberg, L. Sandlund, P. Nordblad, P. Svedlindh, and L. Lundgren, *Phys. Rev. B.* 38 (1988) 7097.
- [46] V. Dupuis, E. Vincent, J.-P. Bouchaud, J. Hammann, A. Ito, and H. Aruga Katori, *Phys. Rev. B.* 64 (2001) 174204.
- [47] J. Lago, S. J. Blundell, A. Eguia, M. Jansen, and T. Rojo, *Phys. Rev. B.* 86 (2012) 064414.
- [48] Y. Sun, M. B. Salamon, K. Garnier, and R. S. Averbach, *Phys. Rev. Lett.* 91 (2003) 167206.
- [49] R. Mathieu, P. Jönsson, D. N. H. Nam, and P. Nordblad, *Phys. Rev. B.* 63 (2001) 092401.
- [50] N. Khan, P. Mandal, and D. Prabhakaran, *Phys. Rev. B.* 90 (2014) 024421.
- [51] K. Dey, S. Majumdar, and S. Giri, *Phys. Rev. B.* 90 (2014) 184424.
- [52] V. K. Anand and D. C. Johnston, *Phys. Rev. B* 91 (2015) 184403.
- [53] E. S. R. Gopal, *Specific Heats at Low Temperatures* (Plenum, New York, 1966).